Synthesis, Crystal Structure, and Solid-State NMR Spectroscopy of $K_2[Ga_4(C_2O_4)(PO_4)_4]\cdot 2H_2O$, a New Gallium Phosphatooxalate with an Intersecting Tunnel Structure

Li-Chun Hung,[†] Hsien-Ming Kao,*[,†] and Kwang-Hwa Lii*[,†,‡]

Department of Chemistry, National Central University, Chungli, Taiwan, R.O.C., and Institute of Chemistry, Academia Sinica, Nankang, Taipei, Taiwan, R.O.C.

Received March 23, 2000. Revised Manuscript Received May 26, 2000

A new gallium phosphatooxalate, $K_2[Ga_4(C_2O_4)(PO_4)_4]\cdot 2H_2O$, has been synthesized hydrothermally and characterized by single-crystal X-ray diffraction and solid-state NMR spectroscopy. It crystallizes in the triclinic space group *P-1* (No. 2) with $a = 7.9863(4)$, $b = 8.2458(5)$, and $c = 8.7631(5)$ Å, $\alpha = 116.075(1)°$, $\beta = 100.825(1)°$, and $\gamma = 104.033(1)°$, $V = 473.3(1)$ Å^3, and $Z = 1$. The structure consists of GaO_6 octahedra and GaO_4 tetrahedra connected by coordinating $C_2O_4^{2-}$ and PO_4^{3-} anions to generate intersecting channels in the three-dimensional framework with guest water molecules and the charge compensating K^+ cations within the channels. The water molecules and K^+ cations sites are half occupied. ^{1}H MAS NMR confirms two different sites for water molecules and also shows that one is more mobile than the other. Three ^{31}P resonances at −10.9, −12.3, and −14.9 ppm are observed at room temperature; the resonance at −14.9 ppm splits into two peaks at 375 K. These four ^{31}P resonances, which have nearly the same intensity, result from different local environments due to the ordering of the water molecules and K^+ cations. The information obtained from ^{1}H → ^{31}P CP/MAS experiments provides insight into the interaction between the guest water molecules in the structural tunnels and the phosphates in the framework. ^{71}Ga MAS NMR confirms the presence of four- and six-coordinated Ga atoms.

Introduction

Recently, many research activities have focused on the synthesis of new open-framework metal phosphates owing to their diverse structural chemistry and potential applications.[1] In the context of building open frameworks, it is possible to use organic molecules in the skeleton.[2−7] As compared with inorganic phosphates, the organic molecules have larger sizes of polyhedral centers and a wide variety of means of connection. This idea is currently used by several research groups and leads to a number of phosphatooxalates of Fe,[8−11] V,[12] Al,[13] Ga,[14,15] and In.[16] A tin phosphonate-oxalate was also reported.[17] We have been studying the gallium system and synthesized two interesting compounds. The structure of $[Ga_5(OH)_2(C_{10}H_9N_2)(C_2O_4)(PO_4)_4]\cdot 2H_2O$ consists of GaO_4 tetrahedra and GaO_6 octahedra linked by phosphate and oxalate groups to form two-dimensional sheets between which are the GaO_4N square pyramids, generating tunnels in which the monoprotonated 4,4′-bipyridinium cations reside.[14] $((R)\text{-}C_5H_{14}N_2)_2[Ga_4(C_2O_4)(H_2PO_4)_2(PO_4)_4]\cdot 2H_2O$ possesses a two-dimensional layer structure with diprotonated (*R*)-2-methylpiperazinium cations being located between the layers.[15] It is the first example of a phosphatooxalate containing a chiral organic amine. In our continuing research on the gallium system, we have synthesized a new gallium phosphatooxalate $K_2[Ga_4(C_2O_4)(PO_4)_4]\cdot 2H_2O$ (further denoted as **1**), which adopts a three-dimensional framework structure with the potassium cations and water molecules within the structural tunnels. It is the first phosphatooxalate containing an alkali metal as charge compensating cation.

[†] National Central University.
[‡] Academia Sinica.

(1) Cheetham, A. K.; Ferey, G.; Loiseau, L. *Angew. Chem., Int. Ed. Engl.* **1999**, *38*, 3268, and references therein.
(2) Abrahams, B. F.; Hoskins, B. F.; Michail, D. M.; Robson, R. *Nature* **1994**, *369*, 727.
(3) MacGillivray, L. R.; Subramanian, S.; Zaworotko, M. J. *J. Chem. Soc. Chem. Commun.* **1994**, 1325.
(4) Gardner, G. B.; Venkataraman, D.; Moore, J. S.; Lee, S. *Nature* **1995**, *374*, 792.
(5) Yaghi, O. M.; Li, G.; Li, H. *Nature*, **1995**, *378*, 703.
(6) Gutschke, S. O. H.; Molinier, M.; Powell, A. K.; Winpenny, R. E. P.; Wood, P. T. *J. Chem. Soc., Chem. Commun.* **1996**, 823.
(7) Hagrman, P. J.; Hagrman, D.; Zubieta, J. *Angew. Chem., Int. Ed. Engl.* **1999**, *38*, 2638, and references therein.
(8) Lin, H.-M.; Lii, K.-H.; Jiang, Y.-C.; Wang, S.-L. *Chem. Mater.* **1999**, *11*, 519.
(9) Lethbridge, Z. A. D.; Lightfoot, P. *J. Solid State Chem.* **1999**, *143*, 58.
(10) Choudhury, A.; Natarajan, S.; Rao, C. N. R. *J. Solid State Chem.* **1999**, *146*, 538.
(11) Choudhury, A.; Natarajan, S. *J. Mater. Chem.* **1999**, *9*, 3113.
(12) Tsai, Y.-M.; Wang, S.-L.; Huang, C.-H.; Lii, K.-H. *Inorg. Chem.* **1999**, *38*, 4183.
(13) Lightfoot, P.; Lethbridge, Z. A. D.; Morris, R. E.; Wragg, D. S.; Wright, P. A.; Kvick, Å.; Vaughan, G. B. M. *J. Solid State Chem.* **1999**, *143*, 74.
(14) Chen, C.-Y.; Chu, P. P.; Lii, K.-H. *J. Chem. Soc. Chem. Commun.* **1999**, 1473.
(15) Lii, K.-H.; Chen, C.-Y. *Inorg. Chem.*, in press.
(16) Huang, Y.-F.; Lii, K.-H. *J. Chem. Soc., Dalton Trans.* **1998**, 4085.
(17) Adair, B.; Natarajan, S.; Cheetham, A. K. *J. Mater. Chem.* **1998**, *8*, 1477.

10.1021/cm000255b CCC: $19.00
Published on Web 07/27/2000

NMR spectroscopy has often been used as a complementary analytical technique with respect to X-ray diffraction methods in the structural elucidation of open-framework materials. For example, in zeolite structure analysis, the long-range periodicity of the silicate framework is analyzed with X-ray diffraction techniques, whereas the local symmetry of the framework and the ordering of guest and adsorbed species are examined with NMR techniques. It is now well established that the resolution obtainable in the magic angle spinning (MAS) NMR spectra of solids is often sufficient to resolve signals from crystallographically distinct atoms. Further, it is possible to resolve resonances from crystallographically equivalent atoms that have different local environments. For gallophosphates, ^{1}H, ^{31}P, and ^{71}Ga NMR experiments are ideally suited to probe the mobility of the intercalated water and to investigate the local environments of ^{31}P and ^{71}Ga nuclei in the framework. In particular, ^{71}Ga NMR is becoming an important tool for structural investigation of inorganic gallium compounds,[18−22] although ^{71}Ga ($I = {}^{3}/_{2}$, 39.6% natural abundance) has a fairly large quadrupole moment ($Q = 1.1 \times 10^{-29}$ m^2) which gives rise to quite broad NMR signals for the central transition in powders because of second-order quadrupolar interaction. In our previous study of $[Ga_5(OH)_2(C_{10}H_9N_2)(C_2O_4)(PO_4)_4]\cdot 2H_2O$, ^{71}Ga MAS NMR spectroscopy confirms the presence of four-, five- and six-coordinate Ga atoms in the structure.[14] In this paper a combined use of single-crystal X-ray diffraction, TGA, and ^{71}Ga, variable-temperature ^{1}H and ^{31}P MAS NMR spectroscopies was employed to probe the local environment of the guest water molecules and the K^+ cations.

Experimental Section

Synthesis and Initial Characterization. In a typical hydrothermal synthesis, a mixture of $Ga(NO_3)_3\cdot 4H_2O$, $C_2H_2O_4\cdot 2H_2O$, $(C_4H_9)_4NCl$, KOH, H_3PO_4, and H_2O in the molar ratio of 1:5:3:7:5:278 was sealed in a Teflon-lined acid digestion bomb and heated at 165 °C for 3 days followed by slow cooling at 10 °C h^{-1} to room temperature. The resulting product consists of colorless rod crystals of **1** in 61% yield based on Ga. The product is monophasic as judged by the total consistency of its X-ray powder pattern with that simulated from the atomic coordinates derived from the single-crystal X-ray study. We have also carried out retrosynthesis without $(C_4H_9)_4NCl$; the resulting product contains crystals of **1** in smaller sizes. Energy-dispersive X-ray fluorescence spectroscopy of several rod crystals confirms the presence of K, Ga, and P. Elemental analysis of C and H contents is consistent with the stoichiometry. (Anal. Found: C, 2.86; H, 0.47. Calcd: C, 2.79; H, 0.465). Thermogravimetric analysis (TGA), using a Perkin-Elmer TGA7 thermal analyzer, was performed on a powder sample in flowing oxygen atmosphere in the temperature range of 30−900 °C with a heating rate of 10 °C min^{-1}. To determine the thermal stability of **1**, a sample was heated to 400, 425, and 450 °C, kept there for 3 h for each temperature, and cooled to room temperature, followed by powder X-ray diffraction using a Siemens D5000 powder diffractometer with Cu Kα radiation. Ion-exchange experiment was performed by stirring **1** with 3 M NH_4Cl(aq) at 50 °C overnight. Elemental analysis of the ion-exchanged product showed that the K^+ cations were not replaced by NH_4^+ in a significant amount.

Single-Crystal X-ray Diffraction. A colorless rod crystals of **1** with the dimensions 0.52 × 0.45 × 0.1 mm was mounted on a Siemens Smart-CCD diffractometer equipped with a normal focus, 3 kW sealed-tube X-ray source. Intensity data were collected in 1271 frames with increasing ω (width of 0.30° per frame). The orientation matrix and unit cell dimensions were determined by a least-squares fit of 4069 reflections. Octants collected and $2\theta_{max}$: $-10 \le h \le 9$, $-10 \le k \le 10$, $-11 \le l \le 11$, 56.5°. Number of measured reflections, unique reflections, and observed unique reflections [$I > 2\sigma(I)$]: 4561, 2044, and 2008. Empirical absorption corrections were performed by using the SADABS program for Siemens area detector ($T_{min,max}$: 0.415, 0.981). On the basis of statistics for intensity distribution and successful solution and refinement of the structure, the space group was determined to be *P-1* (No. 2). The structure was solved by direct methods. The Ga and P atoms were first located, and the C and O atoms were found in difference Fourier maps. The K(1), K(2), and water oxygen (Ow(1) and Ow(2)) sites have an occupancy factor of 0.5. The final cycles of least-squares refinement converged at R1 = 0.0453 and wR2 = 0.1221. The final difference Fourier maps were flat ($\Delta\rho_{max,min}$ = 0.96, −0.99 e/Å^3). Neutral-atom scattering factors for all atoms were used. Anomalous dispersion and secondary extinction corrections were applied. All calculations were performed using SHELXTL programs.[23]

Solid-State NMR Measurements. All NMR experiments were performed on a Bruker AVANCE-400 spectrometer, equipped with a Bruker 4 mm probe, with resonance frequencies for ^{1}H, ^{31}P, and ^{71}Ga of 400.13, 161.73, and 121.84 MHz, respectively. For the ^{1}H MAS NMR experiments, pulse lengths of 4 μs (90° flip angle) and recycle delays of 4 s were used. Pulse lengths of 2.5 μs (45° flip angle) and recycle delays of 40 s were found to be adequate for quantitatively reliable ^{31}P MAS NMR spectra under conditions of high-power proton decoupling. To obtain quantitatively meaningful determinations of quadrupolar nuclei such as ^{71}Ga, a short (<15°) and powerful pulse (an rf field strength of 93 kHz) was used to uniformly excite the sample. To avoid any overlap of the spinning sidebands, ^{71}Ga NMR signals were recorded with a 2.5 mm probe at a spinning speed of 30 kHz. Simulations of ^{71}Ga MAS NMR spectra were performed with the WINFIT program of the Bruker WINNMR software package. Chemical shifts of ^{1}H, ^{31}P, and ^{71}Ga were externally referenced to tetramethylsilane (TMS), 85% H_3PO_4, and $Ga(H_2O)_6^{3+}$ in 1 M $Ga(NO_3)_3$(aq), respectively. The Hartmann−Hahn condition for ^{1}H to ^{31}P cross-polarization (CP) experiments was set on $(NH_4)_2HPO_4$. ^{1}H → ^{31}P CP/MAS spectra were recorded as a function of the contact time ranging from 0.1 to 40 ms.

Results and Discussion

Thermogravimetric Analysis. TGA data for **1** in oxygen show a sharp weight loss of 4.34% which begins at ca. 100 °C and is complete by 150 °C (Figure 1). This weight loss corresponds to the loss of the guest water molecules (4.18% calculated for two H_2O molecules per formula unit). A further weight loss of 8.18% occurs in two overlapping steps between 500 and 600 °C, which can be attributed to the decomposition of oxalate (8.36% calculated for one CO_2 and one CO molecule). Powder X-ray diffraction of the samples that had been heated in air and then cooled in a desiccator revealed that compound **1** retains its structure intact at 400 °C and decomposes at 425 °C.

Description of the Structure. The crystallographic data are summarized in Table 1. The atomic coordinates

(18) Timken, H. K. C.; Oldfield, E. *J. Am. Chem. Soc.* **1987**, *109*, 7669.
(19) Axon, S. A.; Huddersman, K.; Klinowski, J. *Chem. Phys. Lett.* **1990**, *172*, 398.
(20) Massiot, D.; Farnan, I.; Gautier, N.; Trumeau, D.; Trokiner, A.; Coutures, J. P. *Solid State Nucl. Magn. Reson.* **1995**, *4*, 241.
(21) Bradley, S. M.; Howe, R. D.; Kydd, R. A. *Magn. Reson. Chem.* **1993**, *31*, 883.
(22) Fredoueil, F.; Massiot, D.; Poojary, D.; Bujoli-Doeuff, M.; Clearfield, A.; Bujoli, B. *J. Chem. Soc. Chem. Commun.* **1998**, 175.
(23) Sheldrick, G. M. *SHELXTL Programs*, Version 5.1; Bruker AXS, 1998.

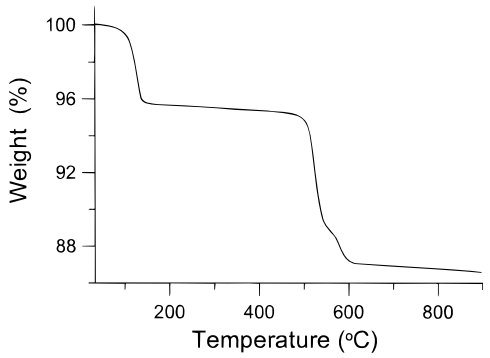

Figure 1. The TGA curve for **1** in flowing air at 10 °C min^{-1}.

Table 1. Crystallographic Data for $K_2[Ga_4(C_2O_4)(PO_4)_4]\cdot 2H_2O$

fw	861.01
cryst syst	triclinic
space group	*P-1* (No. 2)
a, Å	7.9863(4)
b, Å	8.2458(5)
c, Å	8.7631(5)
α, deg	116.075(1)
β, deg	100.825(1)
γ, deg	104.033(1)
volume, $Å^3$	473.3(1)
Z	1
D_{calcd}, g cm^{-3}	3.021
μ, mm^{-1}	65.2
T, °C	22
λ, Å	0.71073
R1[a]	0.0453
wR2[b]	0.1221
GOF	1.361

[a] $R1 = \sum||F_o| - |F_c||/\sum|F_o|$ for $F_o > 4\sigma(F_o)$. [b] $wR2 = \{\sum[w(|F_o|^2 - |F_c|^2)^2]/[w(|F_o|^2)^2]\}^{1/2}$ for all data, where $w = 1/[\sigma^2(F_o^2) + 7.12P]$ and $P = [\max(F_o^2,0) + 2F_c^2]/3$.

Table 2. Atomic Coordinates and Thermal Parameters ($Å^2$) for $K_2[Ga_4(C_2O_4)(PO_4)_4]\cdot 2H_2O$

atom	*x*	*y*	*z*	U_{eq}[a]
K(1)[b]	0.8053(8)	0.4964(7)	0.0434(7)	0.039(1)
K(2)[b]	0.843(1)	0.517(2)	0.373(1)	0.037(2)
Ga(1)	0.3223(1)	0.2169(1)	0.1838(1)	0.0103(2)
Ga(2)	−0.2275(1)	0.0382(1)	0.4964(1)	0.0109(2)
P(1)	0.5445(2)	0.3091(2)	0.5860(2)	0.0102(4)
P(2)	−0.0404(2)	−0.0000(2)	0.2336(2)	0.0101(4)
O(1)	0.6379(7)	0.5176(7)	0.7368(7)	0.017(1)
O(2)	0.5132(7)	0.2827(8)	0.3987(7)	0.015(1)
O(3)	0.3614(7)	0.2202(7)	0.6083(7)	0.015(1)
O(4)	0.6694(7)	0.2020(8)	0.6188(7)	0.017(1)
O(5)	−0.1460(7)	−0.1487(8)	0.0370(7)	0.017(1)
O(6)	0.1266(7)	0.1659(7)	0.2718(7)	0.015(1)
O(7)	0.0148(7)	−0.1128(8)	0.3238(7)	0.015(1)
O(8)	−0.1675(7)	0.0929(8)	0.3276(7)	0.014(1)
O(9)	0.6816(7)	0.0639(8)	−0.0733(7)	0.017(1)
O(10)	0.5288(7)	0.2405(8)	0.0732(7)	0.016(1)
C(1)	0.5602(9)	0.088(1)	−0.0008(9)	0.012(1)
Ow(1)[b]	0.894(3)	0.476(3)	0.045(3)	0.056(5)
Ow(2)[b]	0.887(4)	0.505(5)	0.398(5)	0.041(7)

[a] U_{eq} is defined as one-third of the trace of the orthogonalized U_{ij} tensor. [b] The occupancy factor is 0.5. Ow represents the oxygen atom of a water molecule.

and bond lengths are given in Tables 2 and 3, respectively. All atoms are at general positions. Ga(1) is octahedrally coordinated by phosphate and oxalate groups. Ga(2) is tetrahedrally coordinated by phosphates. If the maximum cation−anion distance, 3.30 Å, as suggested by Donnay and Allmann is considered as interacting,[24] then both K(1) and K(2) are seven-coordinated by phosphate, oxalate, and water oxygens. Bond-valence calculations[25] indicate that both Ga atoms are trivalent and all of the phosphate oxygen atoms have valence sums close to 2. The values for K(1) and K(2) are significantly smaller than 1, indicating that they are loosely bound. Both Ow(1) and Ow(2) form stronger hydrogen bonds with $P(2)O_4$ relative to $P(1)O_4$, as indicated from the O···O distances in Table 3. Ow(2) is observed from a comparison of its thermal parameters with those of Ow(1) to be more strongly bound.

Table 3. Selected Interatomic Distances (Å) for $K_2[Ga_4(C_2O_2)(PO_4)_4)]\cdot 2H_2O$[a]

K(1)−O(1) a	2.866(7)	K(1)−O(4) a	3.191(7)
K(1)−O(5) b	2.884(7)	K(1)−O(7) b	2.846(7)
K(1)−O(9)	3.073(7)	K(1)−O(10)	2.800(7)
K(1)−Ow(2)	3.02(4)	K(2)−O(2)	2.98(1)
K(2)−O(3) c	2.98(1)	K(2)−O(6) c	2.97(1)
K(2)−O(7) b	3.28(1)	K(2)−O(8) c	3.15(1)
K(2)−O(10)	2.81(1)	K(2)−Ow(1)	2.87(2)
Ga(1)−O(1) c	1.902(5)	Ga(1)−O(2)	1.946(5)
Ga(1)−O(5) d	1.919(5)	Ga(1)−O(6)	1.906(5)
Ga(1)−O(9) e	2.070(5)	Ga(1)−O(10)	2.075(5)
Ga(2)−O(3) f	1.826(5)	Ga(2)−O(4) g	1.802(5)
Ga(2)−O(7) f	1.840(5)	Ga(2)−O(8)	1.835(5)
P(1)−O(1)	1.507(5)	P(1)−O(2)	1.519(5)
P(1)−O(3)	1.558(5)	P(1)−O(4)	1.550(5)
P(2)−O(5)	1.509(5)	P(2)−O(6)	1.519(5)
P(2)−O(7)	1.549(5)	P(2)−O(8)	1.559(5)
C(1)−C(1) e	1.54(1)	C(1)−O(9)	1.264(9)
C(1)−O(10)	1.250(9)	Ow(1)···O(7) b	2.94(2)
Ow(2)···O(2)	3.10(4)	Ow(2)···O(6) c	3.02(4)
Ow(2)···O(8) c	3.03(4)	Ow(2)···O(8) h	3.07(4)

[a] Symmetry codes: (a) $x, y, z - 1$; (b) $x + 1, y + 1, z$; (c) $-x + 1, -y + 1, -z + 1$; (d) $-x, -y, -z$; (e) $-x + 1, -y, -z$; (f) $-x, -y, -z + 1$; (g) $x - 1, y, z$; (h) $x + 1, y, z$.

The structure of **1** consists of a 3-dimensional network of $Ga(1)O_6$, $Ga(2)O_4$, $C_2O_4^{2-}$, and PO_4^{3-} moieties with each Ga atom bound to either six or four oxygens, which are, in turn, bound to carbon and phosphorus atoms forming the network. The oxalate anions act as a bis-bidentate ligand to Ga(1)'s to form dimers, which are connected by phosphate tetrahedra to form layers in the (0−11) plane. The oxalate-bridging dimer is also found in other gallium phosphatooxalates. The $Ga(2)O_4$ tetrahedra, positioned between the layers, join the phosphates from adjacent layers, generating intersecting channels parallel to the [100] and [001] directions (Figure 2). Within the channels along either direction are eight-membered rings formed by the edges of 2 GaO_6 octahedra, 2 GaO_4 tetrahedra, and 4 phosphate tetrahedra. The charge compensating K^+ cations and H_2O molecules are located in the eight-membered channels. K(1) and Ow(1) are at the intersections of the channels, whereas K(2) and Ow(2) are within the channels parallel to [001]. All the potassium and water oxygen sites are half-occupied. The short K(1)···Ow(1) distance of 0.77 Å and the short K(2)···Ow(2) distance of 0.44 Å allow us to propose that K(1) and Ow(2) are not simultaneously present with K(2) and Ow(1) in the structural tunnels within a unit cell. This proposal is supported by ^{31}P MAS NMR study (vide infra).

^1H MAS NMR. Two ^1H resonances at 3.5 and 7.2 ppm were observed for the as-synthesized sample at room temperature (Figure 3a). The resonance at 3.5 ppm

(24) Donnay, G.; Allmann, R. *Am. Mineral.* **1970**, *55*, 1003.
(25) Brown, I. D.; Altermann, D. *Acta Crystallogr.* **1985**, *B41*, 244.

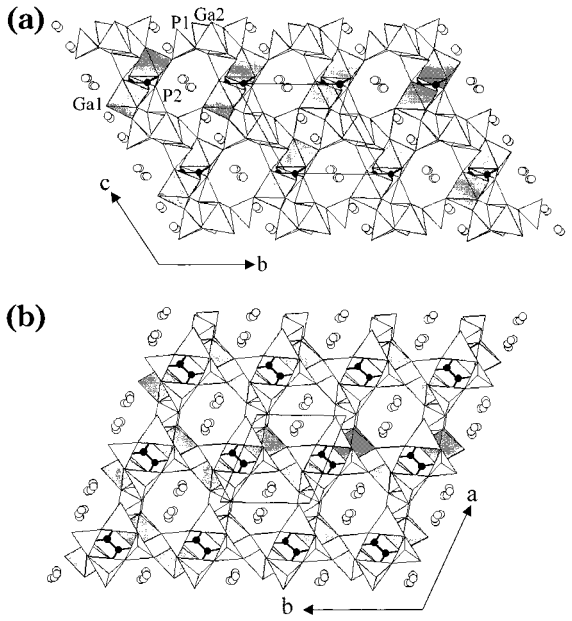

Figure 2. Structure of **1** viewed along (a) the [100] direction and (b) the [001] direction. Polyhedra with dark shading, light shading, and without shading are GaO_6 octahedra, GaO_4 tetrahedra, and PO_4 tetrahedra, respectively. Solid circles, C atoms; stippled circles, K atoms; open circles, water oxygen atoms.

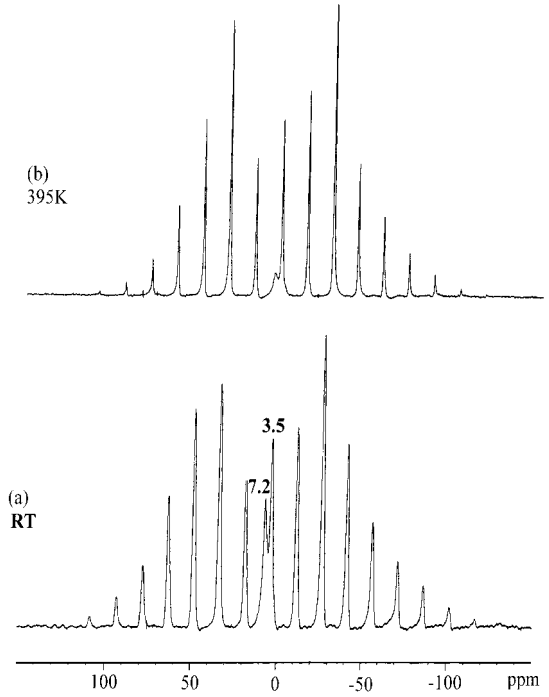

Figure 3. ^{1}H MAS NMR spectra of **1** collected at room temperature and 395 K, at a spinning speed of 6 kHz. The isotropic resonances are labeled at room temperature. All other peaks are spinning sidebands.

associates with a large spinning sideband manifold with the spectral appearance similar to a homonuclear "Pake doublet",[26] spanning about 100 kHz. The width of the sideband manifold is consistent with the size of the ^{1}H−^{1}H dipolar coupling between the two hydrogen atoms in H_2O molecules, and thus the resonance is assigned to molecular H_2O that is structurally bound to the

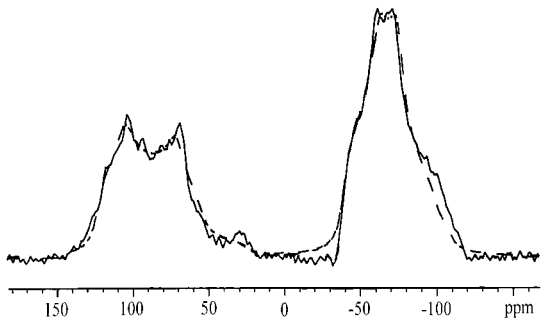

Figure 4. Experimental ^{71}Ga MAS NMR spectrum (solid line) of **1** collected at room temperature at a spinning speed of 30 kHz. The dashed line represents the simulated spectrum using the parameters in Table 4.

phosphate network, corresponding to Ow(2) in the structure. This behavior has been predicted earlier on the basis of the inhomogeneous character of the dipolar interaction in isolated homonuclear two-spin systems.[27,28] Thus, the ^{1}H resonance at 3.5 ppm indicates that the water molecules are isolated rather than clustered, with little intermolecular homonuclear dipolar coupling. These water molecules form a network of hydrogen bonds with the phosphate groups and are not free to undergo translational motion and molecular reorientations in the time scale of the ^{1}H−^{1}H dipolar coupling. The slight asymmetry in the spinning sideband pattern may be explained by the chemical shift anisotropy (CSA) due to molecular water involving hydrogen bonding. It was found that the CSA for rigid water is sizable, approximately 20 ppm (8000 Hz at 400 MHz).[29] The sideband pattern for this resonance does not show any dramatic difference even at 395 K (Figure 3b). In contrast, there are no spinning sidebands associated with the resonance at 7.2 ppm. The lack of spinning sidebands for the resonance at 7.2 ppm suggests that this resonance arises from water molecules undergoing rapid reorientation on the NMR time scale at room temperature. The most plausible assignment for this resonance is to Ow(1), for which the X-ray data indicate larger thermal vibrational amplitude. The intensity of the resonance at 7.2 ppm decreases with increasing temperature as shown in Figure 3b. Ow(1) leaves the framework first as the sample is heated because it is loosely bound at the intersection of channels.

^{71}Ga MAS NMR. Figure 4 shows the experimental ^{71}Ga MAS NMR spectrum of **1** at 9.4 T, obtained at a spinning speed of 30 kHz, together with the simulation. The spectrum displays two well-resolved powder patterns spread ranging from 50 to 150 ppm and −10 to −100 ppm, corresponding to four-coordinate Ga(2) and six-coordinate Ga(1), respectively. There has been a well-established and confirmed correlation that links gallium and aluminum chemical shifts for 4- and 6-fold coordination in silicates, phosphates, zeolites, and organic complexes.[30] The observed line shapes of ^{71}Ga spectrum can be fitted by assuming that they are only

(26) Pake, G. E. *J. Chem. Phys.* **1948**, *16*, 327.

(27) Maricq, M. M.; Waugh, J. S. *J. Chem. Phys.* **1979**, *70*, 3300.
(28) Yesinowski, J. P.; Eckert, H. *J. Am. Chem. Soc.* **1988**, *110*, 1367.
(29) Haeberlen, U. *High-Resolution NMR in Solids*; Academic: New York, 1976; p 149.
(30) Bradley, S. M.; Howe, R. S.; Kydd, R. A. *Magn. Reson. Chem.* **1993**, *31*, 883.

Table 4. Experimental Values for Chemical Shift and Electric Field Gradient for 1

	δ_{iso}[a]	C_Q[b]/MHz	η[c]
^{IV}Ga(2)	129.8	4.97	0.31
^{VI}Ga(1)	−38.7	3.97	0.65

[a] Chemical shifts are referenced to ^{71}Ga resonance in a 1 M gallium nitrate solution; error in the measured value ±10 ppm. [b] Quadrupolar coupling constant ($C_Q = e^2qQ/h$); error in the measured value ±0.25 MHz. [c] Asymmetry parameter.

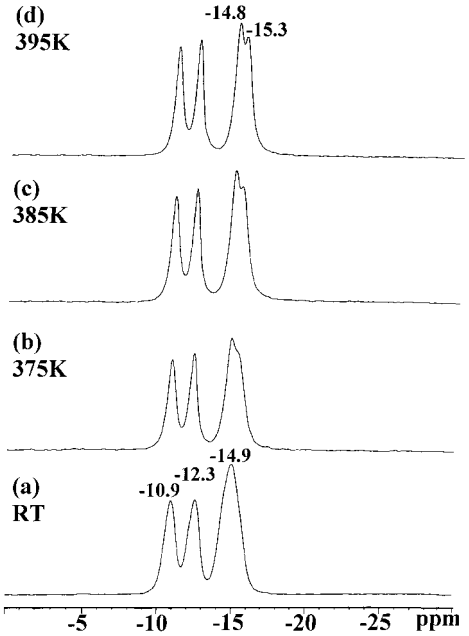

Figure 5. Variable-temperature proton-decoupled ^{31}P NMR spectra of **1** collected at room temperature, 375, 385, and 395 K, at a spinning speed of 12 kHz. The isotropic resonances are labeled at room temperature. The resonance at −14.9 ppm splits into two peaks at −14.8 and −15.3 ppm at 395 K.

influenced by second-order quadrupolar broadening as CSA is averaged by sample spinning. The results obtained from the simulation of the observed ^{71}Ga spectrum, which are summarized in Table 4, not only confirm the presence of four- and six-coordinated Ga atoms but also provide the respective electric field gradient tensors for these two Ga sites that characterize the asymmetry of their local environments. The intensity ratio of Ga(1) to Ga(2) is approximately 1.0:1.2, which is in reasonably good agreement with the X-ray analysis results that the two types of Ga are the same in number per unit cell.

^{31}P MAS NMR with Proton Decoupling. Figure 5a shows the high-power proton-decoupled ^{31}P NMR spectrum obtained at room temperature. There are three ^{31}P resonances at −10.9, −12.3, and −14.9 ppm; the signal intensity of −14.9 ppm is nearly equal to the sum of the intensities of −10.9 and −12.3 ppm. These values agree well with chemical shift range found for other gallophosphates reported in the literature.[31−34] For microporous gallophosphates, chemical shifts in the range from −10 to −20 ppm generally correspond to Q^4 groups.[33] Overweg et al. reported that the zinc gallophosphate $NH_4[ZnGa_2P_3O_{12}(H_2O)_2]$ has ^{31}P peaks located at −10.7 and −11.8 ppm.[34] To assign the ^{31}P resonances of **1** valence sums (Σs) of the bonds between K^+ cations and phosphate oxygen atoms were calculated. The results are summarized as follows: Σ*s*[K(1)−O] = 0.27 for P(2) and 0.19 for P(1); Σ*s*[K(2)−O] = 0.25 for P(2) and 0.20 for P(1). We conclude that $P(2)O_4$ coordinates more strongly to the K^+ cations compared with $P(1)O_4$. Therefore, the resonances at −10.9 and −12.3 ppm are assigned to P(2), on the basis of the downfield chemical shift values due to the deshielding effects from nearby K^+ cations, and the resonance at −14.9 ppm to P(1). The above assignment is also consistent with their ^{31}P spectral intensities. We also note that resonance at −14.9 ppm has larger line width and more asymmetric line shape compared with the other two resonances. Variable-temperature spectra show that at 375 K this resonance splits into two well-resolved peaks at −14.8 and −15.3 ppm (Figures 5b−d). These four ^{31}P resonances have nearly equal intensities. The better spectral resolution of the resonance at −14.9 ppm at high temperature most likely results from the absence of the mobile water molecule Ow(1). The positions of the resonances at −10.9 and −12.3 ppm do not change with the water content except that a slight decrease in line widths was also observed at 375 K.

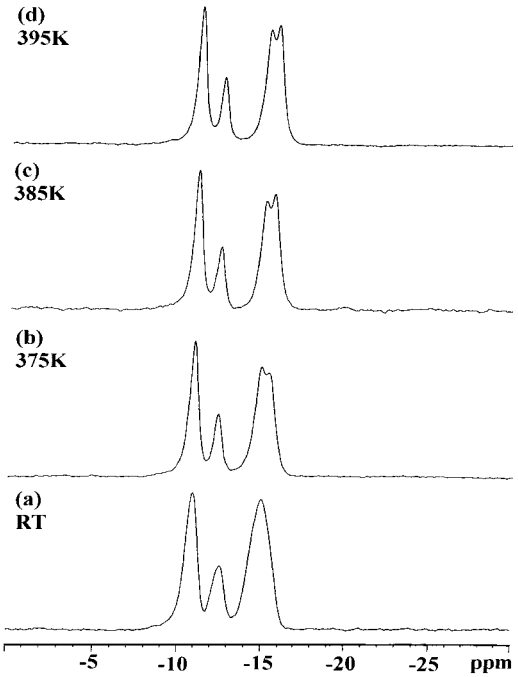

Figure 6. Variable-temperature ^{1}H → ^{31}P CP/MAS spectra (contact time = 2.5 ms) of **1** collected at room temperature, 375, 385, and 395 K, at a spinning speed of 6 kHz.

^{1}H → ^{31}P CP NMR. Variable contact time ^{1}H → ^{31}P CP experiments were also performed to probe the proximity of the protons in the molecular water to framework phosphorus atoms. The variable temperature ^{1}H → ^{31}P CP/MAS spectra of **1** are shown in Figure 6. Figure 7 shows contact time dependence of the four ^{31}P signal intensities at 385 K. The resonances at −10.9, −14.8, and −15.3 ppm have very close hydrogen atoms that can give rise to a fast rising transfer of magnetiza-

(31) Merrouche, A.; Patarin, J.; Kessler, H.; Soulard, M.; Delmotte, L.; Guth, J. L. *Zeolites* **1992**, *12*, 226.
(32) Bradley, S. M.; Howe, R. S.; Hanna, J. V. *Solid-State Nucl. Magn. Reson.* **1993**, *2*, 37.
(33) Reinert, P.; Patarin, J.; Loiseau, T.; Ferey, G.; Kessler, H. *Microporous Mesoporous Mater.* **1998**, *22*, 43.
(34) Overweg, A. R.; de Haan, J. W.; Magusin, P. C. M. M.; van Santen, R. A.; Sankar, G.; Thomas, J. M. *Chem. Mater.* **1999**, *11*, 1680.

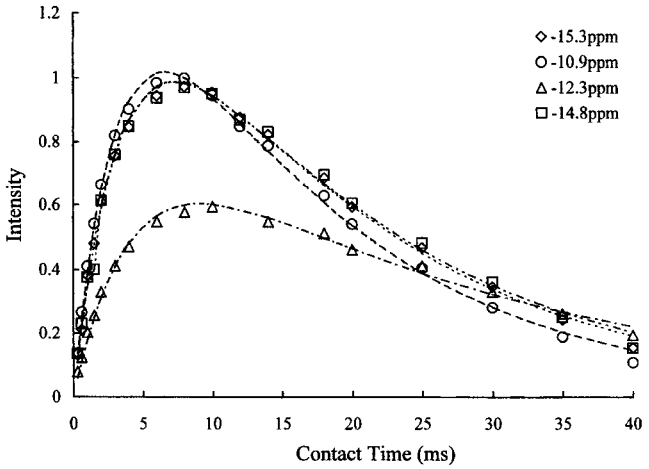

Figure 7. The evolution of $^1H \rightarrow {}^{31}P$ CP signal intensities as a function of the contact time, obtained at 385 K. The dashed line is calculated using eq 1 with the parameters in Table 5.

Table 5. Fitted Parameters of $^1H \rightarrow {}^{31}P$ Cross-Polarization (see Figure 6) at Room Temperature and 385 K

^{31}P sites	−10.9 ppm	−12.3 ppm	−14.8 ppm[a]	−15.3 ppm[a]
		room temperature		
T_{HP}/ms	1.29 ± 0.03	2.83 ± 0.04	1.85 ± 0.03	1.85 ± 0.03
$T_{1\rho}$(H)/ms	41.5 ± 3.5	56.1 ± 4.0	45.0 ± 3.0	45.0 ± 3.0
		385 K		
T_{HP}/ms	3.38 ± 0.05	4.19 ± 0.06	3.59 ± 0.05	3.72 ± 0.05
$T_{1\rho}$(H)/ms	15.4 ± 1.5	26.4 ± 2.0	18.3 ± 1.8	17.5 ± 1.5

[a] These two resonances overlap and give rise to a broad peak at −14.9 ppm at room temperature (see text).

tion due to a large $^1H-{}^{31}P$ dipolar coupling. In contrast a relatively slow transfer of magnetization was observed for the resonance at −12.3 ppm. The curves were analyzed using the following equation[35]

$$M(t) = C[\exp(-t/T_{1\rho}(H)) - \exp(-t/T_{HP})](1 - T_{HP}/T_{1\rho}(H))^{-1} \quad (1)$$

where $M(t)$ is the signal intensity, C is a constant of proportionality, $T_{1\rho}(H)$ is the ^1H spin−lattice relaxation time in the rotating frame, and T_{HP} is the cross relaxation time between the ^1H and ^{31}P spins. The difference in ^{31}P signal intensities obtained from CP generally indicates different T_{HP} values for the corresponding phosphorus species. T_{HP} is related to the strength of the dipolar coupling between ^1H and ^{31}P nuclei. Variations in T_{HP} result from more or less efficient polarization transfers due to differences in dipolar coupling between the nearby water molecules and the corresponding phosphorus species. The experimental data at both room temperature and 385 K have been fitted to eq 1, and the results are listed in Table 5. The cross relaxation time T_{HP} values obtained at 385 K are 3.38, 4.19, 3.59, and 3.72 ms for the resonances at −10.9, −12.3, −14.8, and −15.3 ppm, respectively. The larger T_{HP} value for the resonance at −12.3 ppm indicates poorer signal transfer efficiency from proton spins, suggesting that the water molecule is probably too mobile and/or too far from framework to transfer their polarization to the phosphorus nuclei. This resonance is assigned to the P(2) on the basis of the valence sums of the bonds between K^+ cations and phosphate oxygen atoms. Because K(1) and Ow(2) are not simultaneously present with K(2) and Ow(1) in the structural tunnels within a unit cell, the $P(2)O_4$ tetrahedron which coordinates to K(2) is H-bonded to Ow(1) only. Since the water molecule Ow(1) is mobile, a poor signal transfer from proton spins is expected, and therefore, a larger T_{HP} value is observed for this resonance. In contrast the fast signal transfer at short contact times for the resonance at −10.9 ppm indicates that this phosphate is close to Ow(2), which is more strongly bound to phosphate oxygens. We conclude that the resonances at −10.9 and −12.3 ppm are ascribed to P(2) in close proximity to K(1) and Ow(2), and K(2) and Ow(1), respectively. Similar trend in T_{HP} was also observed at room temperature. In addition, the ^{31}P relaxation times in the rotating frame, $T_{1\rho}(P)$, are nearly identical with a value of 6.8 ms. There is only a minor difference in the T_{HP} and $T_{1\rho}(H)$ values for the resonances at −14.8 and −15.3 ppm. The small difference in the values of chemical shift, T_{HP} and $T_{1\rho}(H)$ of these two resonances indicates that these two resonances are due to P(1) sites with very similar ^{31}P local environments. In contrast to the high-power proton decoupled ^{31}P spectra (Figures 5c and d), the CP signal intensity of the −14.8 ppm resonance is slightly smaller than that of the −15.3 ppm resonance (Figures 6c and d). This implies that the latter is in closer proximity to the molecular water compared with the former.

Conclusions

The hydrothermal synthesis of the three-dimensional organic−inorganic mixed framework material $K_2[Ga_4(C_2O_4)(PO_4)_4]\cdot 2H_2O$ and its crystal structure have been described in this work. The compound is the first phosphatooxalate which contains an alkali metal as charge compensating cation. The structure contains intersecting eight-ring channels in which half-occuplied water molecule and K^+ cations sites are located. ^1H, ^{31}P, and ^{71}Ga MAS NMR experiments have been performed to probe the mobility of the guest water molecules and to investigate the local environments of ^{31}P and ^{71}Ga nuclei in the framework. ^1H MAS NMR confirms two different sites for water molecules and indicates that Ow(1) leaves the framework first as the sample is heated. The results obtained from the simulation of the observed ^{71}Ga spectrum not only confirm the presence of four- and six-coordinated Ga atoms but also provide the respective electric field gradient tensors for these two Ga sites. ^{31}P resonances are assigned on the basis of the interaction between the phosphate oxygen atoms and K^+ cations. A better resolution of the resonance at −14.9 ppm at high temperature can be attributed to the loss of the mobile water molecule. Variable contact time $^1H \rightarrow {}^{31}P$ CP experiments provide further information about the interaction between the guest water molecules in the structural tunnels and the phosphates in the framework.

We aim to combine the flexibility of metal organic coordination systems with the thermal stability of the phosphate materials to produce new open frameworks. Further research in this area by the use of different template species and alternative organic ligands is in progress.

(35) Hayashi, S.; Akiba, E. *Chem. Phys. Lett.* **1994**, *226*, 495.

Acknowledgment. The authors thank the National Science Council and Chinese Petroleum Co. for financial support, Ms. F.-L. Liao and Prof. S.-L. Wang at National Tsing Hua University for X-ray data collection, and Ms. R.-R. Wu at National Cheng Kung University for NMR spectra measurements.

Supporting Information Available: Tables of complete crystal data, atomic coordinates, bond distances and angles, anisotropic thermal parameters, and observed and calculated structure factors (PDF). This material is available free of charge via the Internet at http://pubs.acs.org.

CM000255B